

## UB CCD PHOTOMETRY OF THE OLD, METAL-RICH, OPEN CLUSTERS NGC 6791, NGC 6819, AND NGC 7142

G. CARRARO<sup>1,5</sup>, A. BUZZONI<sup>2</sup>, E. BERTONE<sup>3</sup>, AND L. BUSON<sup>4</sup>

<sup>1</sup> European Southern Observatory, Alonso de Cordova 3107, Casilla 19001, Santiago 19, Chile; [gcarraro@eso.org](mailto:gcarraro@eso.org)

<sup>2</sup> INAF-Osservatorio Astronomico di Bologna, Via Ranzani 1, I-40127 Bologna, Italy; [alberto.buzzoni@oabo.inaf.it](mailto:alberto.buzzoni@oabo.inaf.it)

<sup>3</sup> INAOE-Instituto Nacional de Astrofísica Óptica y Electrónica, Calle L.E. Erro 1, 72840 Tonantzintla, Puebla, Mexico; [ebertone@inaoep.mx](mailto:ebertone@inaoep.mx)

<sup>4</sup> INAF-Osservatorio Astronomico di Padova, Vicolo Osservatorio 5, I-35122 Padova, Italy; [lucio.buson@oapd.inaf.it](mailto:lucio.buson@oapd.inaf.it)

Received 2013 January 25; accepted 2013 August 8; published 2013 October 11

### ABSTRACT

We report on a UV-oriented imaging survey in the fields of the old, metal-rich open clusters NGC 6791, NGC 6819, and NGC 7142. With their super-solar metallicity and ages  $\gtrsim 3\text{--}8$  Gyr, these three clusters represent both very near and ideal stellar aggregates to match the distinctive properties of the evolved stellar populations, as in elliptical galaxies and bulges of spirals. Following a first discussion of NGC 6791 observations in an accompanying paper, here we complete our analysis, also presenting for NGC 6819 and NGC 7142 the first-ever  $U$  CCD photometry. The color–magnitude diagram of the three clusters is analyzed in detail, with special emphasis on the hot stellar component. We report, in this regard, one new extreme horizontal-branch star candidate in NGC 6791. For NGC 6819 and 7142, the stellar luminosity function clearly points to a looser radial distribution of faint lower main sequence stars, either as a consequence of cluster dynamical interaction with the Galaxy or as an effect of an increasing fraction of binary stars toward the cluster core, as also observed in NGC 6791. Compared to a reference theoretical model for the Galaxy disk, the analysis of the stellar field along the line of sight of each cluster indicates that a more centrally concentrated thick disk, on a scale length shorter than  $\sim 2.8$  kpc, might better reconcile the lower observed fraction of bright field stars and their white-dwarf progeny.

*Key words:* binaries: general – stars: horizontal-branch – white dwarfs

*Online-only material:* color figures, supplemental data

### 1. INTRODUCTION

Old open clusters are widely recognized as valuable tools to study the stellar population of the Galactic thin disk (Bragaglia & Tosi 2006; Carraro et al. 2007) and, at the same time, as important benchmarks to probe stellar structure and evolution theories. Recently, much attention has been paid to the evolution of stars along the red giant branch (RGB), and the role of metallicity as a main driver of mass loss (e.g., van Loon 2006; Origlia et al. 2007) and possible origin of extended blue horizontal-branch (BHB) stars. In this context, old, metal-rich, open clusters are ideal targets and, among these, NGC 6791 certainly stands out for its conspicuous population of BHB stars (Kaluzny & Rucinski 1995; Brown et al. 2006) and a wealth of white dwarfs (WDs; Bedin et al. 2008). However, the lack of high-quality UV photometry, particularly in the  $U$  band, has so far prevented a full characterization of the BHB component both in terms of completeness and UV properties.

This is the main scope of the present study, in which we present accurate wide-field  $UB$  photometry across the cluster NGC 6791. This photometric material provided the reference for Buzzoni et al. (2012) to characterize the UV properties of this cluster leading to the conclusion that it can robustly be considered as a nearby proxy of the elliptical galaxies displaying a strong UV-upturn phenomenon. However, a detailed description of the photometric data and their reduction and calibration was deferred to the present paper. Together with NGC 6791, we are going to present here  $UB$  photometry for two additional old, likely metal-rich, open clusters, namely NGC 6819 and NGC 7142, for which CCD  $U$  photometry is not yet available. The main aim is to describe the color–magnitude

diagram (CMD) in these passbands and assess the possible presence of BHB candidate stars.

#### 1.1. NGC 6791

Besides NGC 188, NGC 6791 is the only relatively close system known to contain a sizable fraction of sdB stars (Landsman et al. 1998). Located less than 5 kpc away (Carraro et al. 1999, 2006; Carney et al. 2005), it stands out as a treasured “Rosetta Stone” to assess the UV emission of more distant ellipticals (Buzzoni et al. 2012). Although the first detailed study of NGC 6791 goes back to the work of Kinman (1965), its truly peculiar hot horizontal-branch (HB) content was first recognized a few decades later, when Kaluzny & Udalski (1992, hereafter KU92) and Kaluzny & Rucinski (1995, hereafter KR95) verified that it hosts a significant fraction of sdB/O stars. Later, Yong & Demarque (2000) interpreted these hot sources as extreme horizontal-branch (EHB) stars with  $T_{\text{eff}}$  in the range of 24–32,000 K, as also confirmed by ground and space-borne (UIT and *HST*) observations (Liebert et al. 1994; Landsman et al. 1998).

Its old age, about 8 Gyr, has recently been confirmed by Anthony-Twarog et al. (2007) using  $vbyCaH\beta$  CCD photometry, while a recent estimate of metallicity (i.e.,  $[\text{Fe}/\text{H}] \sim +0.40$ ) has been provided by Carraro et al. (2006), Origlia et al. (2006), and Gratton et al. (2006), relying on high-resolution spectroscopy.

#### 1.2. NGC 6819

The first hint of the relatively old age of this cluster dates back almost 30 years ago, from the photographic studies of Lindoff (1972) and Auner (1974), which compared the turnoff and RGB location relative to the CMD of the evolved system M67. More recent and accurate age estimates from deep *BVI*

<sup>5</sup> On leave from Dipartimento di Fisica e Astronomia, Università di Padova, Italy.

**Table 1**  
Journal of Observations for the 2003 Run

Target	Date	Filter	Exposure (s)	Airmass	Seeing (arcsec)
NGC 6791	2003 Jul 29	<i>U</i>	1200	1.02–1.09	0.8
		<i>B</i>	300	1.01–1.13	0.7
PG2213+006		<i>U</i>	2 × 30	1.14–1.62	0.9
		<i>B</i>	2 × 10	1.14–1.63	0.8
NGC 6819	2003 Jul 30	<i>U</i>	1200	1.02–1.16	0.9
		<i>B</i>	300	1.02–1.18	0.8
PG2213+006		<i>U</i>	2 × 30	1.14–1.62	0.7
		<i>B</i>	2 × 10	1.14–1.63	0.7
NGC 7142	2003 Jul 31	<i>U</i>	1200	1.25–1.28	1.0
		<i>B</i>	300	1.25–1.31	1.0
PG2213+006		<i>U</i>	30	1.14–1.62	0.9
		<i>B</i>	10	1.14–1.63	0.8
PG1525+071		<i>U</i>	30	1.14–1.62	0.9
		<i>B</i>	10	1.14–1.63	0.9

CCD photometry (Carraro & Chiosi 1994; Kalirai et al. 2001; Rosvick & Vandenberg 1998; Warren & Cole 2009) better agree with an age value of  $\sim 3$  Gyr. No *U* photometry has been published so far for this cluster.

Chemical abundances from high-resolution spectroscopy of red-clump stars in the cluster have recently been presented by Bragaglia et al. (2001) and Warren & Cole (2009), suggesting a value of  $[\text{Fe}/\text{H}] = +0.09$ . This consistently agrees with the original estimate by Twarog et al. (1997), based on Strömgren photometry.

### 1.3. NGC 7142

The similarity of the NGC 7142 CMD with that of the old open clusters NGC 188 and M67 has been pointed out by van den Bergh (1962). Specific *BV* CCD photometry has been carried out by Crinklaw & Talbert (1991) pointing to an age of 4–5 Gyr for this cluster, actually intermediate between that of M67 and NGC 188. This estimate matches both the very early observations of van den Bergh (1962) and the more recent results of Carraro & Chiosi (1994). As far as metallicity is concerned in NGC 7142, Jacobson et al. (2007, 2008) ascribe a moderately super-solar metal content, with a value of  $[\text{Fe}/\text{H}] = +0.14$ . The only modern CCD study of this cluster is from Janes & Hoq (2011), on the *BVI* passbands, and supports previous estimates for age, distance, and reddening.

## 2. OBSERVATIONS AND DATA REDUCTION

A first CCD *U, B* observing run was carried out with the highly *U*-sensitive DOLORES optical camera mounted on the 3.6 m Telescopio Nazionale Galileo (TNG) at the Roque de Los Muchachos Observatory of La Palma (Spain). Observations were carried out along the three nights of 2003 July 29–31. DOLORES was equipped with a 2048 × 2048 pixel LORAL CCD with a 0".275 pixel size. This provided a 9".4 × 9".4 field of view on the sky. Four slightly overlapping fields were eventually observed across each cluster, covering a total area of roughly 17'.0 × 17'.0 (see Figure 1). The details of the observations are listed in Table 1. A further set of shallower images with a 5 s exposure time and a similar pointing sequence and instrumental setup has subsequently been required to recover saturation effects in the photometry of the brightest stars ( $B \lesssim 14$ ) in the fields. These supplementary data have been kindly provided for clusters NGC 6819 and 7142 by the TNG service staff along

**Table 2**  
Coefficients for Standard Magnitude Calibration

<i>U</i> Band	$u_1$	$u_2$	$u_3$
Jul 29	$0.341 \pm 0.022$	$0.49 \pm 0.02$	$0.103 \pm 0.033$
Jul 30	$0.349 \pm 0.018$	$0.49 \pm 0.02$	$0.099 \pm 0.023$
Jul 31	$0.367 \pm 0.014$	$0.49 \pm 0.02$	$0.139 \pm 0.018$
<i>B</i> Band	$b_1$	$b_2$	$b_3$
Jul 29	$-1.544 \pm 0.010$	$0.25 \pm 0.02$	$0.022 \pm 0.014$
Jul 30	$-1.581 \pm 0.013$	$0.25 \pm 0.02$	$-0.016 \pm 0.017$
Jul 31	$-1.581 \pm 0.012$	$0.25 \pm 0.02$	$-0.004 \pm 0.016$

with the 2009 October observations. Unfortunately, no useful data have been made available for NGC 6791, so a different correcting procedure had to be devised for this cluster, as we discuss in Section 3.1.

Data have been reduced with the IRAF<sup>6</sup> packages CCDRED, DAOPHOT, ALLSTAR, and PHOTCAL using the point-spread-function method (Stetson 1987). The three nights along the 2003 run turned out to be photometric and very stable, which allowed us to derive calibration equations for all of the 20 observed standard stars of the two Landolt (1992) fields.

The calibration equations turned out to be in the form

$$\begin{aligned} u &= U + u_1 + u_2 * X + u_3(U - B) \\ b &= B + b_1 + b_2 * X + b_3(U - B), \end{aligned} \quad (1)$$

where *U* and *B* are standard magnitudes, *u* and *b* are the instrumental ones, and *X* is the airmass; all of the coefficient values are reported in Table 2. Second-order terms have also been calculated, but turned out to be negligible (0.005–0.015), and therefore are not included.

In the case of NGC 6791, the specific goal of this run was to assess the possible presence of additional hot EHB stars fainter than  $B \sim 17$ , that is the magnitude of the seven, UV-enhanced candidates originally reported by KU92. Quite unexpectedly, the preliminary results of these data led Buson et al. (2006) to suspect the presence of a bright EHB clump of stars surmounting the KU92 objects. However, a closer scrutiny of the reduced data revealed that most of the newly detected candidates in fact displayed too high of a photometric error for their apparent luminosity and were too close to the *B* saturation limit of our deep photometry to provide conclusive arguments on their nature as hot sdB stars.

### 2.1. Cross-check with Other Photometry Sources in the Literature

Cluster NGC 6791 is the only one with independent *UB* photometry carried out by KR95, and this provided a valuable opportunity to check our results by cross-correlating the two photometric catalogs. The comparison was restricted only to stars fainter than  $B = 15.55$  mag, to safely avoid any saturation effect in our magnitude scale. The magnitude and color residuals for the 5510 stars in common with the KR95 data set are shown in Figure 2. In these plots, the displayed difference is in the sense “our photometry”–KR95. As evident from the figure, a fairly good agreement is found for the *B* photometry, with a mean magnitude residual  $\langle \Delta B \rangle = 0.064 \pm 0.041$  over the whole star sample. Major discrepancies appear, on the contrary,

<sup>6</sup> IRAF is distributed by the National Optical Astronomy Observatory, which are operated by the Association of Universities for Research in Astronomy, Inc., under cooperative agreement with the National Science Foundation.

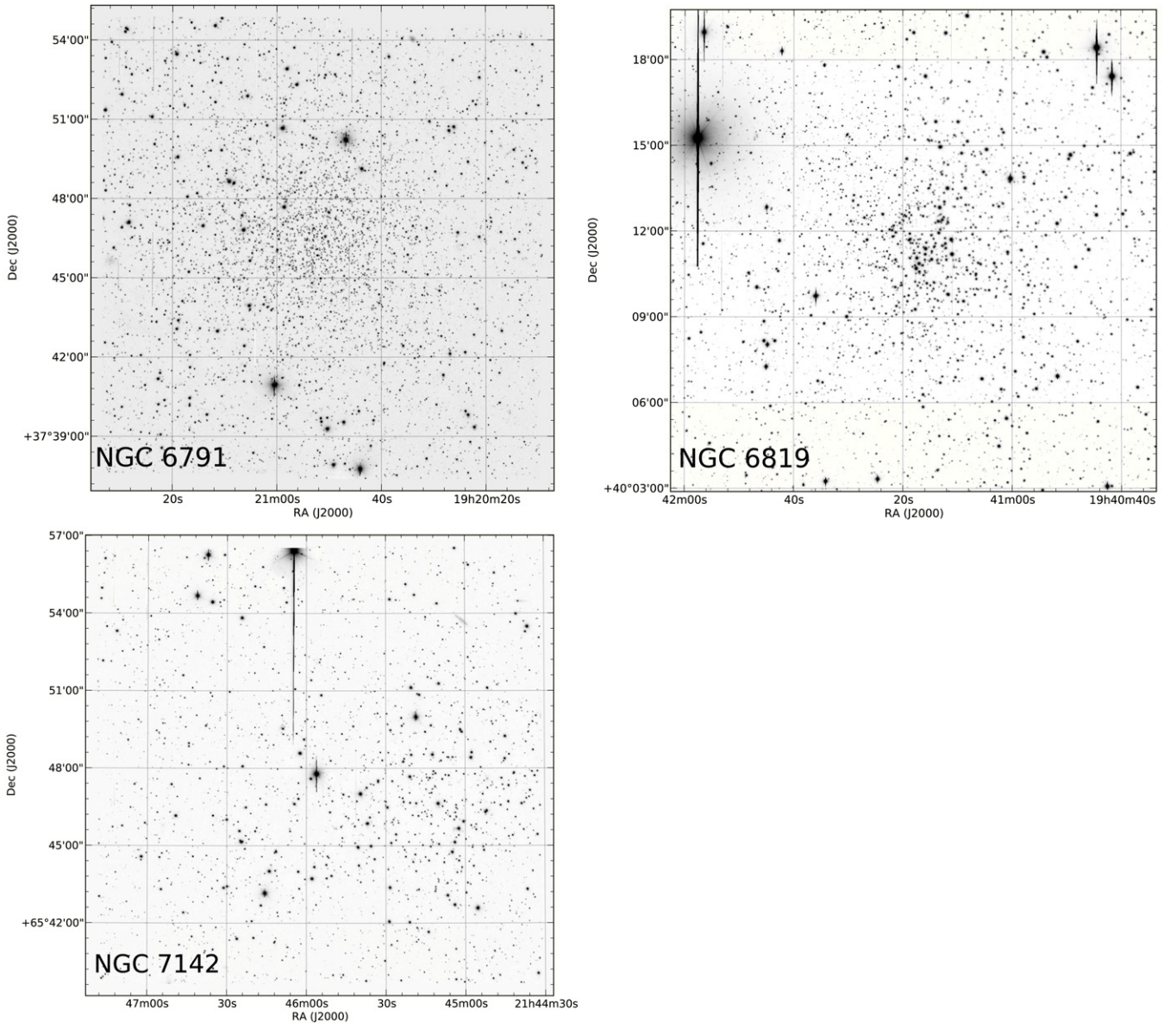


**Figure 1.** B 300 s mosaics of the 4 pointings for each cluster, NGC 6791, NGC 6819, and NGC 7142, as labeled in each panel. The field of view is  $17'$  on a side. North is up, east to the left.

for the  $U$  magnitudes with a larger zero-point offset, namely  $\langle \Delta U \rangle = -0.204 \pm 0.177$ , and a clear evidence of a color drift (see the upper panel of Figure 2). One has to keep in mind, in this regard, that KR95 themselves warn about possible systematics with their  $U$  filter and apply an a posteriori offset to their  $(U - B)$  color.

An independent settlement of this apparent mismatch can be attempted by further cross-correlating our photometry with the CCD magnitudes of Montgomery et al. (1994), as shown in Figure 3. Quite comfortably, the much smaller photometric offsets, i.e.,  $\langle \Delta B \rangle = 0.021 \pm 0.059$  and  $\langle \Delta U \rangle = 0.058 \pm 0.232$ , and the lack of any evident color drift for the 2370 stars in common, confirm the excellent agreement, thus strengthening our photometry results with respect to the KR95 results.

## 2.2. Completeness Analysis

From Table 1, it is obvious that the three clusters have been observed under the same seeing conditions. However,

Figure 1 shows that NGC 6791 is by far the most crowded cluster, and therefore its photometry is the most affected by crowding/incompleteness effects. Both NGC 6819 and NGC 7142 look less affected by this problem. Therefore, we investigated incompleteness effects only on NGC 6791 images. Completeness corrections were determined in the standard way by running artificial star experiments on the data, frame by frame, in both  $U$  and  $B$  filters. Basically, several simulated images were created by adding artificial stars to the original frames. The artificial stars were added at random positions and had the same color and luminosity distribution as the sample of true stars. To cope with potential over-crowding, up to 20% of the original number of stars were added in each simulation. Depending on the frame, between 1500 and 2000 stars were added in this way. The ratio of recovered to inserted stars is a measure of the photometry completeness. The results are summarized in Table 3 and show that both in  $U$  and in  $B$ , the photometry has a completeness value larger than 50% up to 23 mag.

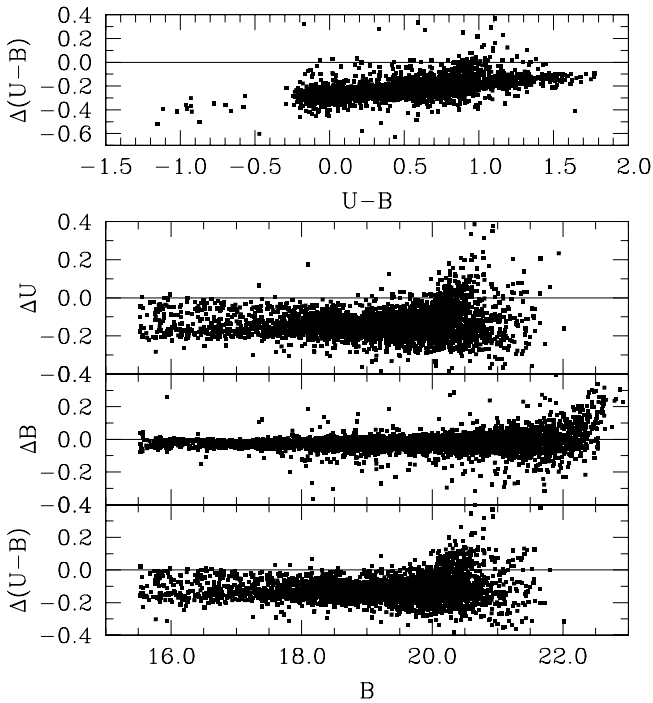


**Figure 2.**  $U$ ,  $B$  cross-correlation of our photometry with KR95 data for cluster NGC 6791. Color and magnitude differences for the 5510 stars in common are displayed in the different panels vs. our photometry. Mean zero-point offsets are in the sense “our photometry”–KR95. Note, in the upper panel, the evident  $(U - B)$  color drift of KR95 photometry with respect to our data.

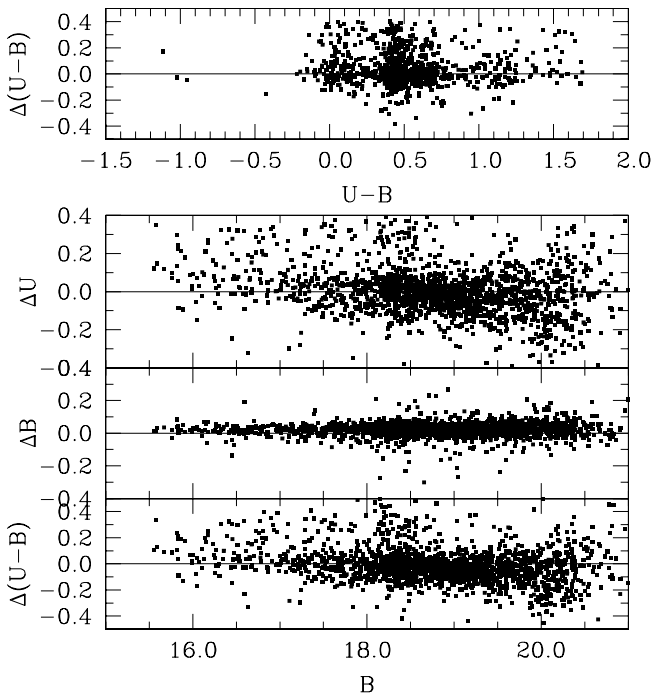


**Figure 3.** Same as Figure 2, but comparing with Montgomery et al. (1994) CCD magnitudes of 2370 NGC 6791 stars in common with our data set. Magnitude residuals are in the sense “our photometry”–Montgomery et al., and are plotted against our photometry. The vanishing residual distribution in the different panels confirms that our photometry is in the same reference as that of Montgomery et al.

**Table 3**  
Completeness Study for NGC 6791 as a Function of the Filter

$\Delta$ Mag	$U$	$B$
13–14	100%	100%
14–15	100%	100%
15–16	100%	100%
16–17	100%	100%
17–18	100%	100%
18–19	100%	100%
19–20	100%	100%
20–21	93%	95%
21–22	84%	85%
22–23	70%	73%
23–24	38%	41%

### 3. CLUSTER CMDs

The DAOPHOT search across the field of our three clusters allowed us to confidently detect and measure magnitude and color for some 18,000 objects brighter than  $B \simeq 24.0$  in the fields of the three clusters. Within these magnitude limits, the NGC 6791 sample consisted of 7774 stars, while 7683 and 3422 stars have been picked up in the NGC 6819 and NGC 7142 fields, respectively. A quick-look analysis of the internal photometric uncertainty of our survey can be carried out by means of Figure 4. From the plots, one can appreciate that  $B \sim 22$  mag has been safely reached throughout, mostly within a 0.05 mag accuracy. The  $B$  versus  $(U - B)$  CMDs for our clusters are presented in Figures 5, 9, and 12.

#### 3.1. NGC 6791

Our output for the NGC 6791 field is shown in Figure 5, where we also compare with the Kaluzny & Rucinski (1995) original photometry (Table 2 therein). As previously mentioned, the two data sets exhibit zero-point differences in  $U$ , which make the Kaluzny & Rucinski (1995) diagram systematically “redder” in  $(U - B)$  color. To overcome our saturation problems with the brightest  $B$  magnitudes, we cross-identified all of our brightest  $B$  magnitude sample with the Kaluzny & Rucinski (1995) catalog, and use the latter source for all  $B \leq 15.55$  mag objects across our field, to correct the Kaluzny & Rucinski (1995) photometry to our magnitude scale according to Figure 2. As a result, the CMD in the right panel of Figure 5 matches our own photometry for stars fainter than  $B = 15.55$  mag, and matches the (revised) Kaluzny & Rucinski (1995) photometry, for the 110 objects brighter than  $B = 15.55$  mag. Overall, our global NGC 6791 catalog consists of 7840 entries and its resulting CMD is consistently the same as in the Buzzoni et al. (2012) analysis. Note from Figure 5 that our photometry turns out to be over one magnitude deeper than Kaluzny & Rucinski (1995) reaching the WD region at the faint-end tail of magnitude distribution, about  $B \sim 22.5$ .

A comparison of our CMD with the YZVAR Padova isochrone set (Bertelli et al. 2008), as shown the right panel of Figure 5, helps us constrain the overall evolutionary properties of the cluster. For a chemical mix  $(Z, Y) = (0.04, 0.30)$ , the observed CMD confirms a consensus age between 6 and 8 Gyr (Anthony-Twarog et al. 2007; Buzzoni et al. 2012) and causes a shift of models to an apparent  $B$  distance modulus  $(m - M)_B = 13.6$  mag, assuming a color excess of  $E(U - B) = 0.13$ .

Also in Figure 5, the 19 hot-star candidates proposed by Kaluzny & Rucinski (1995, see Tables 1 and 2 therein) are

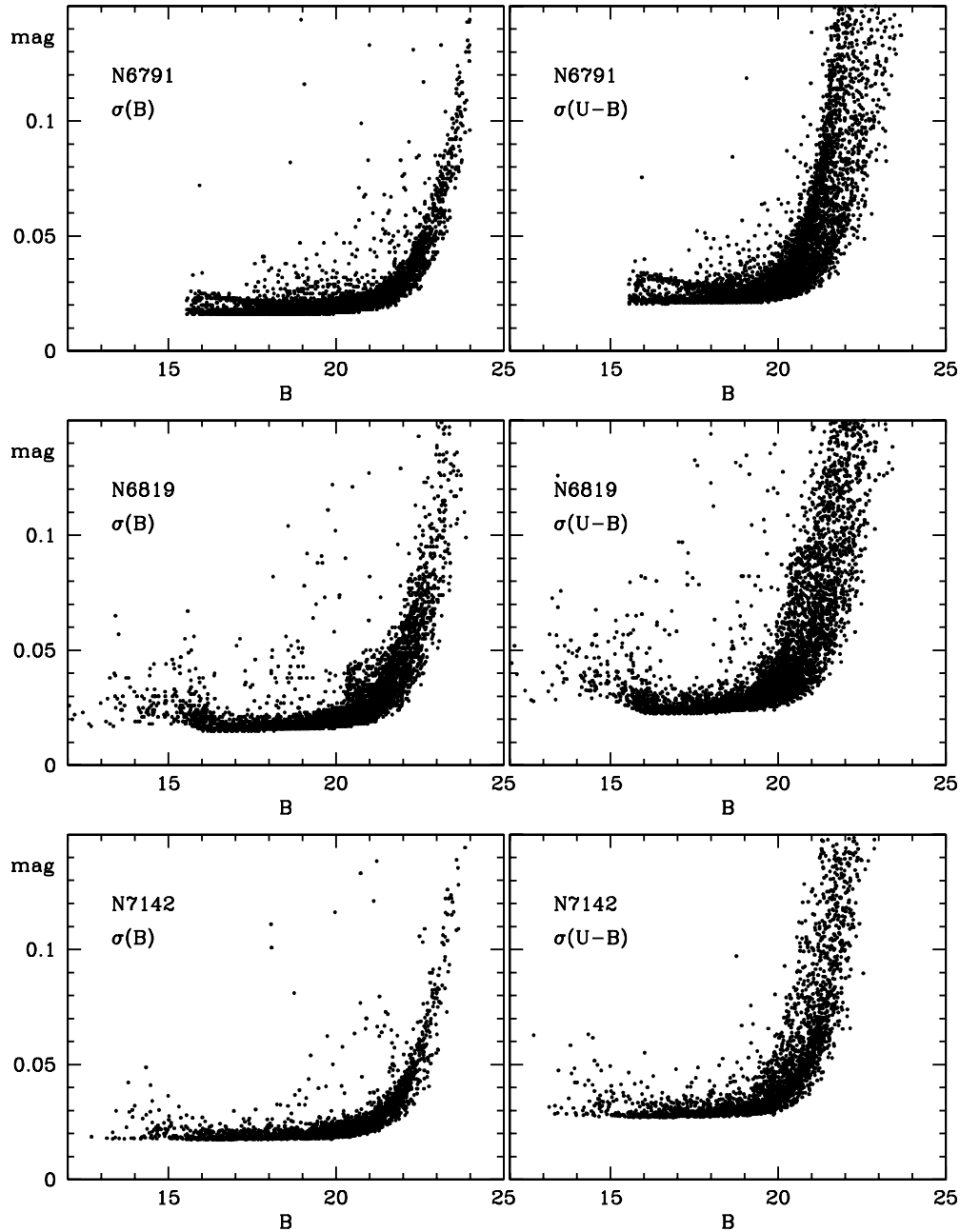


**Figure 4.**  $B$ -band internal errors from DAOPHOT photometry in the field of NGC 6791, NGC 6819, and NGC 7142. Where available, “shallow” imagery has been used for the photometry of the brightest ( $B \lesssim 15.5$ ) stars in the fields of NGC 6819 and 7142, as explained in Section 2. The bright-end star distribution in the NGC 6791 field, on the contrary, has been recovered from KR95 photometry, as discussed in Section 3.1. Note that the  $B \sim 22$  mag level has been safely reached in the three clusters, mostly within a 0.05 mag accuracy.

encircled in both CMDs. The sub-group of WDs fainter than  $B \sim 19.5$  is easily recognized, while an obvious EHB candidate clump stands out around  $B \sim 18$ . Of these, stars B01 and B07 in the Kaluzny & Rucinski (1995) original list are controversial cases, claimed to be field stars by Liebert et al. (1994) according to radial velocity measurements, but recently reclassified as likely members of the cluster by Platais et al. (2011) based on their new astrometric analysis. The case of star B10 is even further controversial, because according to Kaluzny & Rucinski (1995), this object is a blend of two stars with  $\Delta V \sim 2$  mag but is questioned as a likely field interloper by Platais et al. (2011). After careful inspection, object B10 can confidently be resolved in our frames, and we are inclined to assign cluster membership to at least the brightest component of the blend.

Following Buzzoni et al. (2012), one more star should be included in this EHB sample. This is target B08 in the Kaluzny & Rucinski (1995) notation, the most UV-enhanced object in our sample. In spite of its much fainter apparent  $B$  magnitude, in fact, this star is the hottest object in our catalog, which implies a much larger intrinsic luminosity, after bolometric correction, which is fully consistent with its location in the high-temperature extension of the cluster HB (see Figure 3 in Buzzoni et al. 2012). Star B08 was partly excluded in the original CMD of Kaluzny & Rucinski (1995; see the left panel of Figure 5) due to a redder color, mainly in consequence of a  $\sim 1$  brighter  $B$  magnitude, compared to our photometry. Such a notable difference urged a thorough check on our TNG frames to manually probe apparent  $U$  and  $B$  magnitudes. A supplementary check was also carried

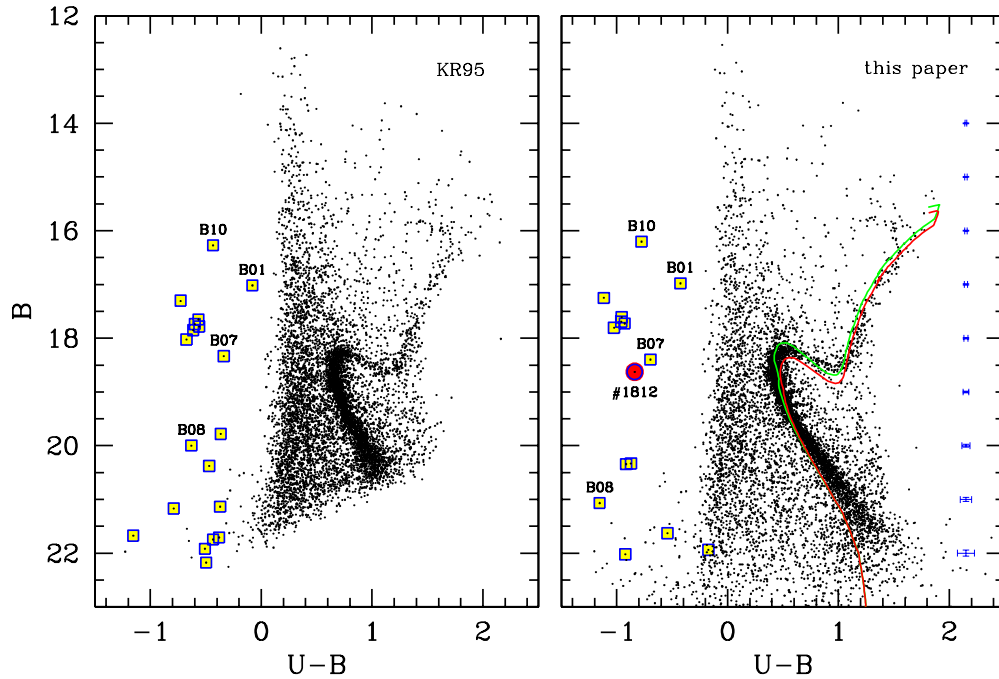


**Figure 5.** Comparison of the  $B$  vs.  $(U - B)$  CMD of NGC 6791 according to Kaluzny & Rucinski (1995; left panel) and the present paper (right panel). The KR95 hot-star candidates of Tables 3 and 4 (including, in particular, the outstanding EHB stellar clump about  $B \sim 18$ ) are marked in both plots as big squares. The three controversial cases of stars B01, B07, and B10 are also labeled in the plots, together with star B08, the hottest object in our sample. The big dot in the right panel indicates the new EHB candidate (ID 1812 in Table 3) we discovered in this study. An illustrative match with the Padova isochrone set (Bertelli et al. 2008) is displayed in the right panel assuming for the cluster an age range between 6 and 8 Gyr and chemical mix  $(Z, Y) = (0.04, 0.30)$ . The theoretical models have been shifted to an apparent  $B$  distance modulus  $(m - M)_B = 13.6$  mag and reddened by  $E(U - B) = 0.13$ . Typical error bars for our photometry at the different magnitude levels are displayed on the right.

(A color version and supplemental data of this figure are available in the online journal.)

**Table 4**  
EHB Candidates in the Field of NGC 6791

ID	R.A. (J2000.0)	Decl.	$B$	$(U - B)$	KR95
NGC 6791					
377	19:20:40.33	37:53:50.9	16.98(0.02)	-0.43(0.03)	B01
411	19:20:49.92	37:41:39.0	17.25(0.02)	-1.12(0.03)	B02
554	19:20:45.19	37:49:31.5	17.61(0.02)	-0.96(0.04)	B03
585	19:21:12.91	37:45:51.3	17.69(0.02)	-0.96(0.04)	B04
606	19:21:03.36	37:46:59.8	17.73(0.02)	-0.93(0.04)	B05
644	19:20:45.34	37:48:19.5	17.80(0.02)	-1.03(0.04)	B06
1379	19:21:07.41	37:47:56.5	18.40(0.02)	-0.70(0.04)	B07
5939	19:20:35.74	37:44:52.3	21.07(0.03)	-1.15(0.05)	B08
156	19:21:01.92	37:50:46.2	16.20(0.01)	-0.78(0.02)	B10
1812	19:20:20.22	37:46:27.6	18.63(0.02)	-0.84(0.04)	...

**Note:** KR95: ID no. from Kaluzny & Rucinski (1995).

out for star B16, which we see  $\sim 0.8$  fainter in  $B$  than Kaluzny & Rucinski (1995). After careful inspection, in both cases we can fully confirm our magnitude estimates in Tables 4 and 5, thus attributing most of the apparent discrepancy to the Kaluzny & Rucinski (1995) photometry.

Overall, according to our survey, we could only detect 14 out of the 19 hot-star candidates of Kaluzny & Rucinski (1995), since 5 of them (namely B09, B12, B13, B17, and B19) happen to fall outside our field of view. The cross-identification of the nine Kaluzny & Rucinski (1995) EHB candidates in our sample is reported in Table 4, together with accurate J2000.0 coordinates,  $B$  magnitude, and  $(U - B)$  color according to our observations. For the reader's convenience, the remaining five stars in our field are summarized in Table 5. The position of all

**Table 5**  
Other Cross-referenced Faint Hot Stars in the Field of NGC 6791, According to Kaluzny & Rucinski (1995)

ID	R.A. (J2000.0)	Decl.	$B$	$(U - B)$	KR95
6684	19:20:30.78	37:51:06.2	21.63(0.03)	-0.54(0.05)	B11
6995	19:20:59.08	37:47:15.1	21.94(0.03)	-0.17(0.05)	B14
4801	19:20:20.90	37:46:57.4	20.34(0.03)	-0.92(0.05)	B15
4784	19:20:44.92	37:46:40.2	20.33(0.03)	-0.87(0.05)	B16
7068	19:20:16.92	37:44:46.2	22.02(0.04)	-0.92(0.06)	B18

**Note:** KR95: ID no. from Kaluzny & Rucinski (1995).

the 14 hot stars in common with Kaluzny & Rucinski (1995) is indicated in the cluster map of Figure 6.

In addition to the nine bona fide EHB stars in the Kaluzny & Rucinski (1995) list, a new candidate that escaped previous detection—i.e., entry 1812 in the present catalog, aka star “c” in Figure 3 of Buzzoni et al. (2012)—should be added to the EHB sample. Its dereddened  $(U - B)$  color suggests a temperature of  $T_{\text{eff}} \simeq 22,300$  K (Buzzoni et al. 2012). This star is reported in Table 4 and marked as a big red dot in our CMD of Figure 5 (right panel) and in the cluster map of Figure 6. A more detailed finding chart, for future observing reference, is also reported in Figure 7. Although not confirmed spectroscopically, the projected distance from the cluster center makes this target compatible with its possible membership to the system. This statistical argument will be further detailed in Section 4, leading us to conclude that this star has a  $>70\%$  membership probability.

Based on our revised star catalog, we also carefully reconsidered the nature of the striking clump of UV-strong stars, about  $B \sim 15.5$ , which first appeared in the CMD of NGC 6791, as

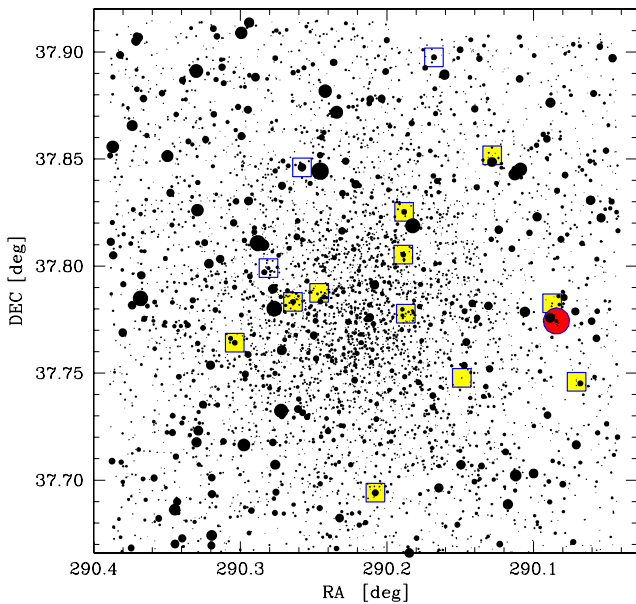


**Figure 6.** New EHB candidate proposed in this study located here on the cluster map of NGC 6791 (big red solid dot) together with the Kaluzny & Rucinski (1995) hot-star sample, as from Figure 5 (square markers). The questioned member stars, B01, B07, and B10, are singled out with open squares.

(A color version of this figure is available in the online journal.)

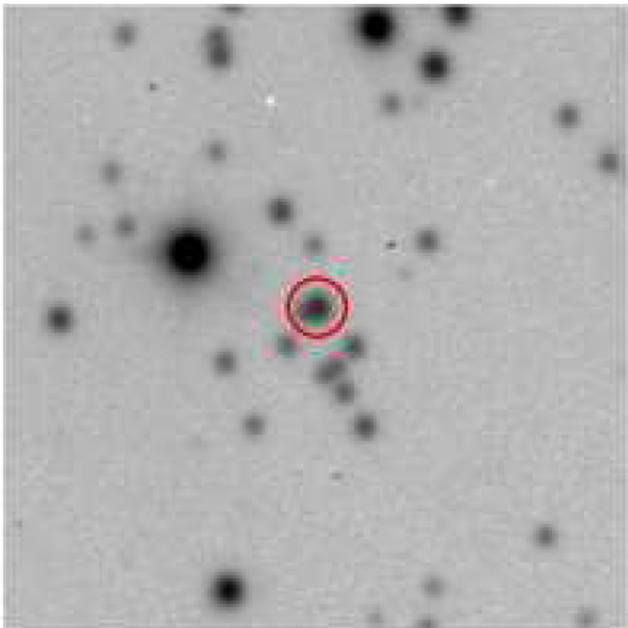


**Figure 7.** *B*-band finding charts for the new EHB candidate in NGC 6791 proposed in this study. This is star ID 1812 in our catalog. Chart is  $1' \times 1'$  across, centered at the coordinates of Table 4. North is up, east is to the left.

(A color version of this figure is available in the online journal.)

shown in Buson et al. (2006, see Figure 2 therein). Although clearly detected on the deep *U* imaging frames, these objects stand out in our original photometric catalog for their large *B* photometric error, a feature that led us to suspect some intervening saturation effect in this band. For this reason, an “ad hoc” individual recognition of this bright sample on the original TNG images has been carried out together with an independent cross-identification of each target in the Kaluzny & Rucinski (1995) *B* catalog. Our perception actually did turn out to be correct, and

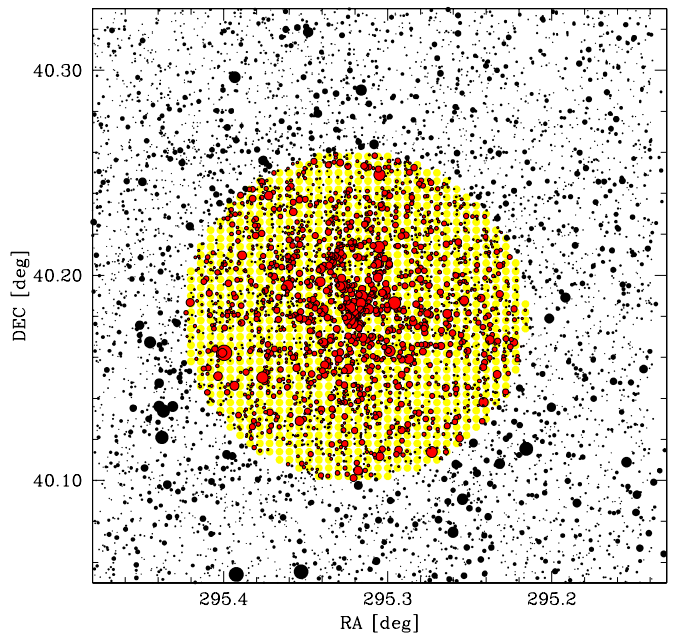


**Figure 8.** Overall map of the surveyed field across NGC 6819. The central spot locates the “inner” region of 5 arcmin radius surrounding the cluster center. Some very bright stars east of the cluster have been masked (see Figure 1) preventing accurate photometry in the relatively close region.

(A color version of this figure is available in the online journal.)

after recovering CCD saturation, we were unable to isolate any additional (clump of) UV-bright stars in NGC 6791.<sup>7</sup>

Overall, across our field of view, the open cluster NGC 6791 seems to host a total of ten EHB stars.

### 3.2. NGC 6819

This study presents the first-ever *U* CCD photometry for NGC 6819. Down to  $B = 24.0$ , our photometric catalog collects a total of 6504 objects. The system looks very concentrated spatially with a substantial fraction of its stellar population comprised within a radius of  $\sim 5'$  from the center (see Figure 8). According to the star number-density distribution, the latter can be located at  $(\alpha; \delta)_{2000.0} \simeq (19^{\text{h}}41^{\text{m}}17^{\text{s}}; +40^{\circ}10'47'')$ .

The CMD of the 2413 stars within the “inner” region (Figure 9, upper panel) shows a well populated stellar main sequence (MS), that neatly shows up against the Galactic background. Also, a red clump of HB stars, about 1 mag brighter than the turn off (TO) point, is clearly visible in the figure, at about  $(U - B) \sim 1.4$ . One can also notice that the TO region displays an evident “hooked” pattern pertinent to stars of  $M \gtrsim 1.4 M_{\odot}$  growing a convective core inside. This is evocative of stellar populations of intermediate age. Actually, a tentative match of the “inner” CMD with the Padova isochrones (Bertelli et al. 2008) for  $(Z, Y) = (0.04, 0.30)$  (see again the upper panel of Figure 9) points to an age of  $\sim 3$  Gyr, after reddening models for a color excess  $E(U - B) = 0.15$  and assuming an apparent *B* distance modulus  $(m - M)_B = 12.0$  mag for the cluster.

Interestingly enough, the MS stellar distribution seems to vanish toward lower luminosities with a clear deficiency of stars fainter than  $B \sim 20$ . A comparison with the observed field star counts, at the same magnitude level, definitely rules out any possible bias due to incomplete sampling and points to

<sup>7</sup> Similarly, the saturation check also led us to reject two additional hot-star candidates of Buzzoni et al. (2012, see labeled objects “a” and “b” of Figure 3 therein).

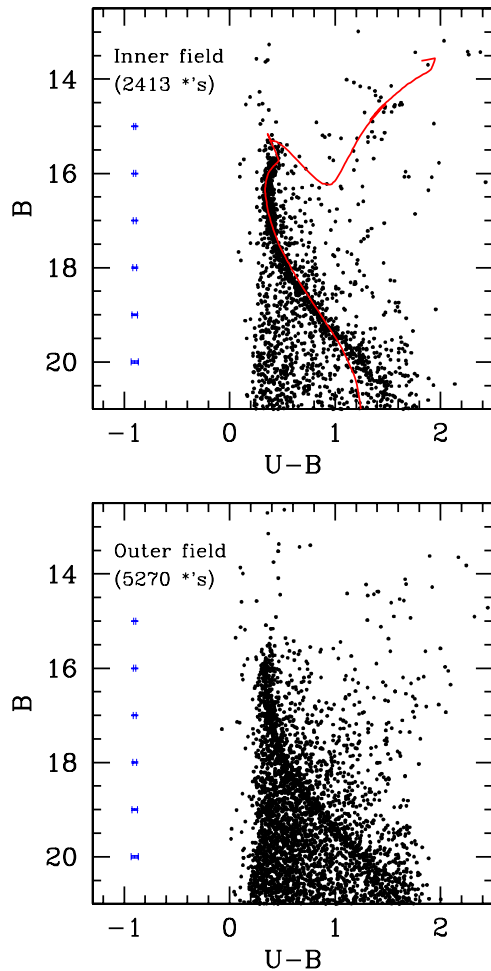


**Figure 9.** Upper panel: the  $B$  vs.  $(U - B)$  CMD of the “inner” region (within  $5'$  from the cluster center) of NGC 6819. A total of 2413 stars brighter than  $B = 24.0$  are displayed, as labeled. Note the “hooked” turn off pattern about  $B \simeq 15.5$  and the red clump of HB stars, about 1 mag brighter, about  $(U - B) \sim 1.4$ . A tentative match with the 3 Gyr Padova isochrone (Bertelli et al. 2008) is displayed for  $(Z, Y) = (0.04, 0.30)$ . We imposed an apparent  $B$  distance modulus  $(m - M)_B = 12.0$  mag and a color excess  $E(U - B) = 0.15$ . Lower panel: same plot but for stars in the “outer” region of the field, that is beyond  $5'$  from cluster center (5270 objects in total, within the same magnitude limit). For both panels, typical error bars for our photometry at the different magnitude levels are displayed on the left.

(A color version and supplemental data of this figure are available in the online journal.)

an inherently “flat” (i.e., giant-dominated, in the mass range  $1.02\text{--}1.17 M_{\odot}$ ) or truncated initial mass function for the cluster stellar population.

Although much more blurred and heavily perturbed by field star interlopers, all of these features of the CMD can also be recognized in the corresponding plot of the 5270 stars across the “outer” region ( $r > 5'$  in Figure 8), as in the lower panel of Figure 9. This clearly points to a much larger extension of the NGC 6819 system itself, as found indeed by Kalirai et al. (2001), who placed the cluster edge  $\sim 9.5$  away from the center.

Once rescaled to the same area across the sky, the apparent luminosity function of the “inner” and “outer” regions in NGC 6819 can consistently be compared, as in Figure 10. Supposing the Galaxy background to be uniformly distributed across the field, then the residual excess of bright red giants and upper-MS stars in the innermost region effectively traces the cluster stellar population. In addition, the plot also confirms that cluster low-MS stars fainter than  $B \sim 20$  are spread out

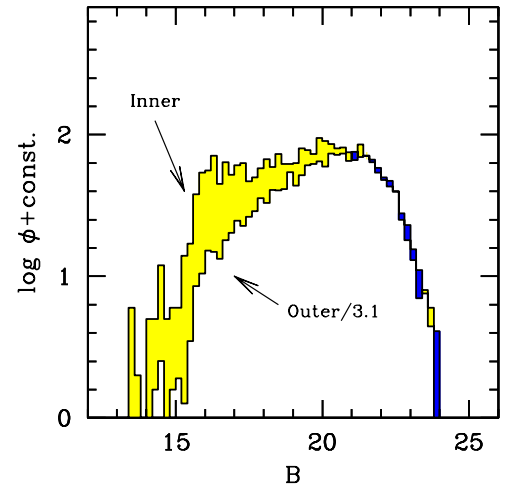


**Figure 10.** Apparent  $B$ -luminosity function of the “inner” and “outer” regions across the NGC 6819 field. To consistently compare the two regions, “outer” star counts have been reduced by a factor of  $\sim 3.1$  to rescale to the same area as for the “inner” region. Note the inner residual excess of bright red giants and upper-MS stars and the lack of any central concentration for the low-MS stellar distribution fainter than  $B \sim 20$ .

(A color version of this figure is available in the online journal.)

across the field and do not show any central concentration. Our evidence fully supports the results of Kalirai et al. (2001), who pointed out the prevailing presence of low-mass stars ( $M \lesssim 0.65 M_{\odot}$ ) in the outer regions of the cluster.

### 3.3. NGC 7142

Similar to NGC 6819, we are also presenting here the first ever  $U$ -band CCD photometry for NGC 7142. A total of 3422 stars brighter than  $B = 24.0$  have been measured. The cluster does not clearly stand against the field and looks very contaminated. This reinforces the idea that NGC 7142 is a loose open cluster on the verge of dissolving into the Galactic disk (van den Bergh & Heeringa 1970).

The stellar locus in the  $B$  versus  $(U - B)$  plane can be enhanced by restraining our display to the densest innermost region of the system. For this reason, we collected stars into a circular region within a  $5'$  radius around the cluster center, the latter assumed to coincide with the peak of the star number density, roughly located at  $(\alpha; \delta)_{2000.0} \simeq (21^{\text{h}}45^{\text{m}}11^{\text{s}}; +65^{\circ}46'49'')$  (see Figure 11). This “inner” sample consists of 1087 stars and evidently maximizes the fraction of cluster members. Its CMD (upper panel of Figure 12) can be contrasted with the “outer” stellar distribution across the surrounding field, amounting to a total of 2335 stars (lower panel of the figure).

The cluster MS neatly appears in the upper panel of the figure, with the TO point located at  $[B, (U - B)] \sim [16.5, 0.3]$ . The MS smoothly connects with a coarse but extended RGB that tips at about  $[B, (U - B)] \sim [14.0, 2.3]$ . As with NGC 6819, the diagnostic match with the Bertelli et al. (2008) Padova isochrones provides very similar results, pointing to an age of roughly 4 Gyr (see upper panel of Figure 12). Similar to NGC 6819, no clear evidence for any possible hot stellar component to be related with the cluster population seems to emerge from the analysis of our CMD.

By further extending the comparison with NGC 6819, a notable feature from the CMDs of Figure 12 is an inherent deficiency of faint low-MS stars below  $B \sim 20$ . This feature becomes even more evident as far as the cluster luminosity function is assessed, although on a merely statistical basis, in



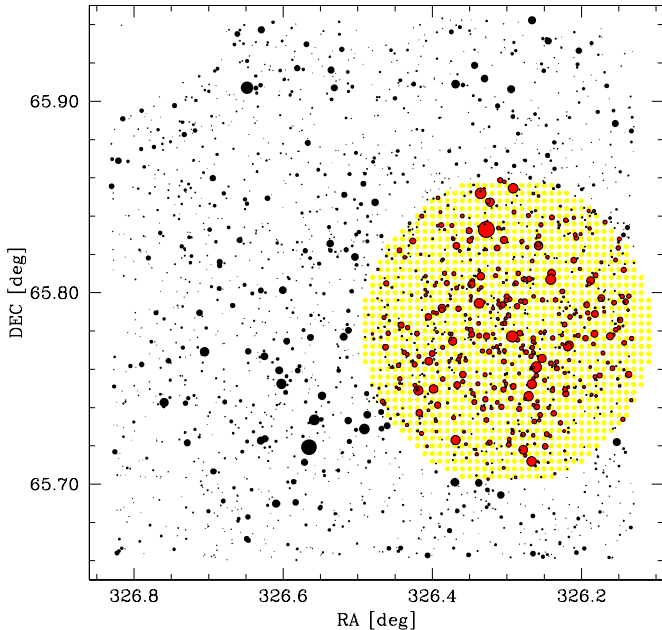


**Figure 11.** Overall map of the surveyed field across NGC 7142. The central spot locates the “inner” region of 5 arcmin radius surrounding the cluster center. A bright star northeast of the cluster has been masked (see Figure 1) thus preventing accurate photometry in the relatively close region.

(A color version of this figure is available in the online journal.)

terms of star count excess versus  $B$  apparent magnitude of the “inner” versus “outer” sample, as shown in Figure 13. Such a vanishing MS, together with the overall loose morphology of the cluster, may consistently fit with a dynamical scenario modulated by the Galaxy interaction. Faint low-mass stars should, in fact, be the first and most affected by Galaxy tidal stripping over the cluster lifetime (McLaughlin & Fall 2008). On the other hand, likewise with NGC 6819, an apparent lack of low-mass stars could also be the tricky by-product of a prevailing fraction of binary (multiple?) stellar systems within the cluster population. If this is the case, then the entire MS locus might be affected, leading, among others, to a younger inferred age for the cluster, as probed by a brighter TO point.

#### 4. CLUSTER MEMBERSHIP AND FIELD STAR CONTAMINATION

As a result of the large covered field and the low ( $b \approx 8^\circ\text{--}11^\circ$ ) Galactic latitude, a substantial fraction of disk stellar interlopers is expected to affect our open-cluster observations. To independently probe the Galaxy contamination along our pointing directions, and eventually assess, on a firmer statistical basis, cluster membership of the observed stars in each cluster, we made a Monte Carlo experiment relying on the Girardi et al. (2005) Galactic model to compute synthetic CMDs of the relevant sky regions. To make our realizations statistically significant, we ran several trials by varying the random seed, and then smeared the synthetic CMDs by adding photometric errors from our observations, according to Figure 4. Finally, reddening at infinity has been applied to the theoretical  $(U - B)$  colors, following Schlegel et al. (1998).

The synthetic field realizations along the line of sight of NGC 6791, 6819, and 7142 are displayed in the three left panels of Figure 14, as labeled on the plots. To ease a direct comparison with the corresponding CMDs of Figures 9 and 12, where lower panels better probe the field in the off-center region

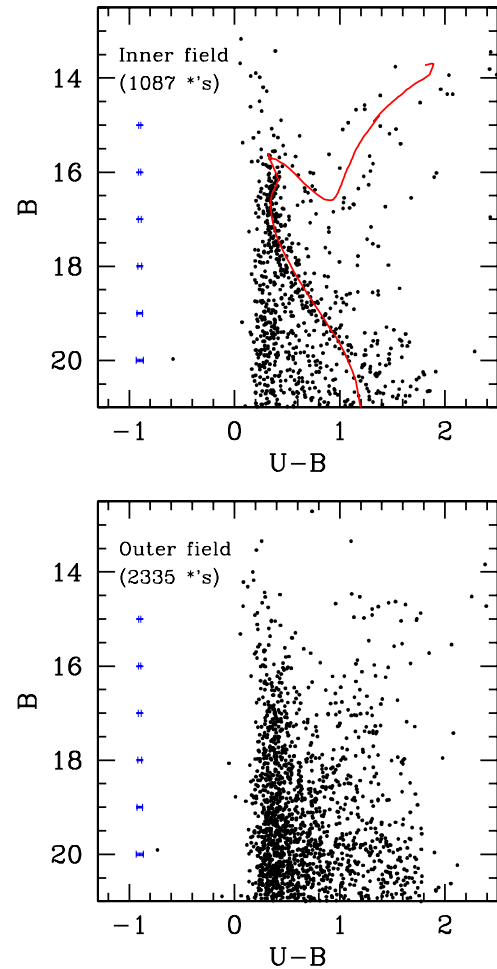


**Figure 12.** Same as for Figure 9, but for cluster NGC 7142. In order to enhance cluster visibility, the upper panel collects photometry for 1087 stars brighter than  $B = 24.0$  in an “inner” region within 5 arcmin from the cluster fiducial center, as in the map of Figure 11, while the field distribution in the “outer” region (2335 stars) is displayed in the lower panel. A match is attempted in the upper panel with a 4 Gyr Padova isochrone (Bertelli et al. 2008) for  $(Z, Y) = (0.04, 0.30)$ . An apparent  $B$  distance modulus  $(m - M)_B = 12.0$  mag and a color excess  $E(U - B) = 0.10$  is assumed to rescale models. For both panels, typical error bars for our photometry at the different magnitude levels are displayed on the left.

(A color version and supplemental data of this figure are available in the online journal.)

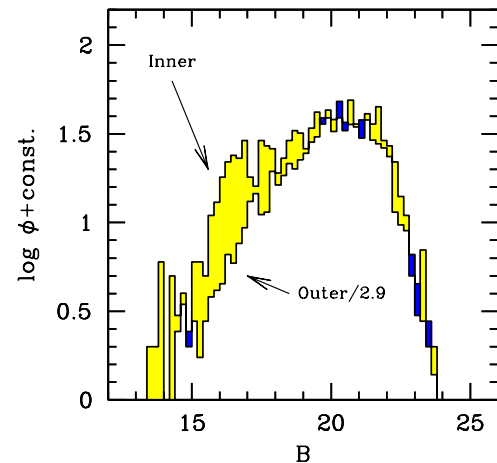


**Figure 13.** Same as for Figure 10, but for cluster NGC 7142. Again, to consistently compare the “outer” and “inner” areas, star counts in the external region have been rescaled by a factor of  $\sim 2.9$ , as labeled in the plot.

(A color version of this figure is available in the online journal.)

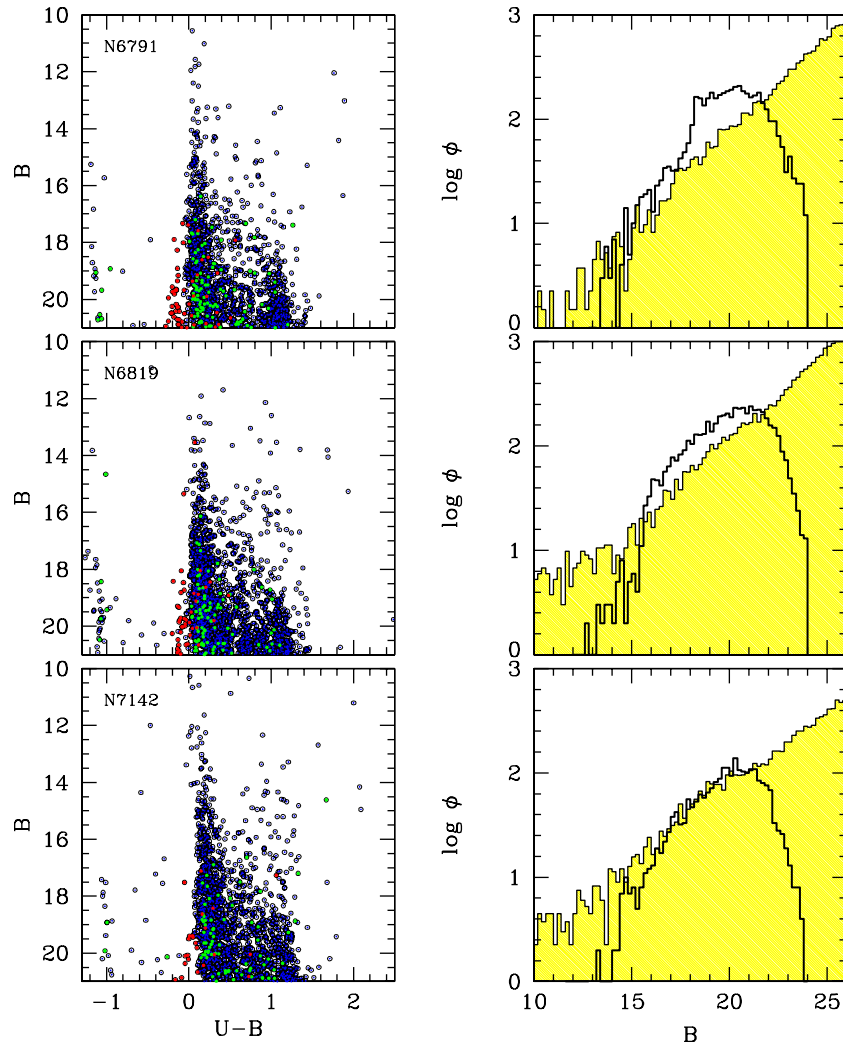


**Figure 14.** Field realizations along the line of sight of NGC 6791, 6819, and 7142 simulated by means of the Girardi et al. (2005) Galactic model. The synthesis output has been scaled throughout to an area of 0.06 square deg in order to consistently match the observed stellar sample of our “outer”-field regions (as in the maps of Figures 8 and 11, for instance). The synthetic CMDs are displayed in the left panels, while the corresponding  $B$ -band luminosity function are computed in the right panels, and compared with our “outer” observations on a similar area of the clusters (thick-line histograms). Color code in the synthetic CMDs is red for halo stars, green for the thin disk, and blue for the thick disk. Note, all the way, the prevailing contribution of thick-disk stars to the coarse Galactic field.

(A color version of this figure is available in the online journal.)

of the clusters, we scaled our simulations to match a similar coverage area on the sky (namely  $\sim 0.06 \text{ deg}^2$ ). The contribution of the different Galaxy components is color coded in the plots of Figure 14, with halo stars in red, thin-disk stars in green, and thick-disk stars in blue. Consistent with the low Galactic latitude of our clusters, one can notice that thick-disk stars are by far the prevailing contributors throughout.<sup>8</sup> For each cluster, in the right panels of Figure 14, we also compared the  $B$ -luminosity functions, as observed across the “outer” regions of the three fields (thick-line histograms overplotted in each panel), with the corresponding Monte Carlo output.<sup>9</sup> As expected, the clusters NGC 6791 and NGC 6819 are easily seen to “spill over” the  $5'$  region in the CMDs of Figures 5 and 9 and induce a star count excess in the field luminosity function. This is not the case for

<sup>8</sup> According to Girardi et al. (2005) an exponential radial density profile is assumed for the thick-disk stellar component in the model, with a scale length of 2.8 kpc.

<sup>9</sup> The same selection is adopted for NGC 6791, for which we probed the  $B$  luminosity function for stars across the map of Figure 6 located  $5'$  or more away from the cluster center, the latter assumed to coincide with the peak of the star number density at  $(\alpha; \delta)_{2000.0} \simeq (19^{\text{h}}20^{\text{m}}52^{\text{s}}; +37^{\circ}46'13'')$ .

NGC 7142 which, on the contrary, seems to be fully contained within the inner  $5'$  spot of Figure 11.

Cluster membership of stars within the “inner” regions of our frames can be statistically assessed by taking advantage of the Milky Way synthetic templates and relying on the Mighell et al. (1998) procedure. Restraining our test to stars brighter than  $B \sim 20$ , we note that, on average, about 78% of the objects in the “inner” region of NGC 6791 can confidently be cluster members. A similar figure is obtained for NGC 6819, leading to a membership fraction of 71% within the inner  $5'$  radius. Due to its vanishing profile, the case of NGC 7142 is much worse, suggesting that the cluster actually consists of a mere 28% of the “inner” stars.

As far as the distinctive properties of the Galaxy field are concerned, at least three interesting differences seem to emerge from the comparison of our “outer” stellar samples and the Girardi et al. (2005) synthesis model of Figure 14. More specifically:

1. Even considering the smearing effect of photometric errors, a much broader extension toward “redder” colors still has

to be reported for our observations, with a larger fraction of faint ( $B \gtrsim 18$ ) objects exceeding  $(U - B) \gtrsim 1.5$ , as shown in the CMDs of Figures 5, 9, and 12. Distant galaxies in the background, like high-redshift ellipticals, may be an issue in this regard as they extend in apparent color to be much redder than Galactic M-type dwarfs. However, differential reddening effects may also cause apparent discrepancy. A check has been carried out by relying on the relative shift of the MS locus in the cluster CMD across the field of view, as explained in von Braun & Mateo (2001). Although no sign of “patched” reddening is found across NGC 6819 and NGC 7142, there exists a rough  $(\Delta E(U - B) \sim \pm 0.1 \text{ mag})$  internal uncertainty of our procedure due to poor statistics. Just marginal (though cleaner) evidence of a reddening gradient appears, on the contrary, for NGC 6791, with hints of  $E(U - B)$  slightly increasing by  $\sim 0.05 \pm 0.04 \text{ mag}$  toward the east edge of the field.

2. As far as the luminosity function is concerned (see the left panels of Figure 14), the bright-end stellar distribution of the Girardi et al. (2005) model tends to predict a more sizeable fraction of very bright ( $B \lesssim 13$ ) (thick-disk) stars, not present in the same amount in our stellar samples.<sup>10</sup>
3. Finally, and even more importantly, an enhanced population of WDs (of both thick- and thin-disk origin) is predicted in all three fields with a clear sequence of faint ( $B \gtrsim 18$ ) UV-strong objects “bluer” than  $(U - B) \sim -1$ . However, observations show no sign of such a sizeable field WD population, at least in the line of sight of NGC 6819 and 7142, while only marginal evidence might perhaps tackle the nature of the few faintest UV stars in NGC 6791. Altogether, points (2) and (3) may hint that the Girardi et al. (2005) theoretical scheme should refine its assumed thick-disk morphology pointing to a shorter scale length, to reduce the overwhelming presence of relatively close (bright) stars and their progeny of WDs in the solar neighborhood.

## 5. SUMMARY AND DISCUSSION

We reported on a multiple, UV-oriented survey in the fields of the open clusters NGC 6791, NGC 6819, and NGC 7142, which—owing to their super-solar metal content and estimated old age—represent both very near and ideal stellar aggregates to match the distinctive properties of the evolved stellar populations, possibly displaying the UV-upturn phenomenon in elliptical galaxies and bulges of spirals. To determine this, we made use of TNG  $U, B$  imagery.

For each cluster, the resulting  $B$  versus  $(U - B)$  CMD fairly well matches the fiducial evolutionary parameters as proposed in recent literature, a fact that further corroborates the quality of our data set. In particular, taking the Padova suite of isochrones as a reference (Bertelli et al. 2008) for TO fitting, and owing to a super-solar metallicity for all three clusters, we confirm for the NGC 6791 stellar population an age of  $7 \pm 1 \text{ Gyr}$ , while slightly younger figures, i.e., 3 and 4 Gyr, may be more appropriate for NGC 6819 and 7142, respectively.

As already pointed out by Landsman et al. (1998), a bimodal HB morphology is clearly confirmed for NGC 6791, where the sizeable population of BHB stars accompanies the standard red clump (RHB) in a relative number partition of  $[\text{BHB} : \text{RHB}] \sim [1 : 4]$ . By relying on the observed HB distribution and

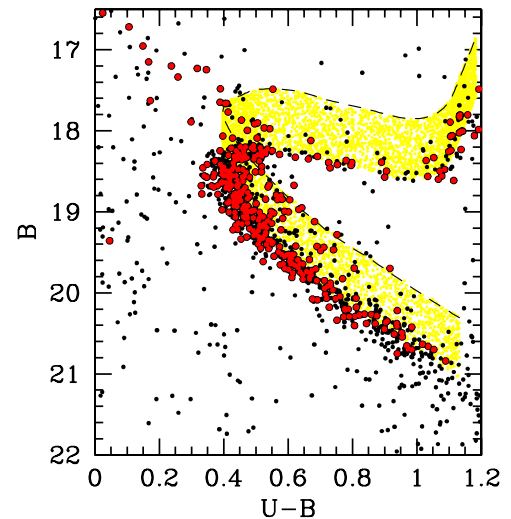


**Figure 15.** Zoomed-in CMD of NGC 6791 around the MS turn-off region. Only stars in our catalog within a  $2.5$  radius from the cluster center have been considered, in order to minimize the field-star contamination. According to K. M. Cudworth (2008, private communication, as cited by Twarog et al. 2011) stars with membership probability  $P_m \geq 80\%$  have been marked by big red dots. The dashed curve is the MS fiducial locus shifted toward  $0.75 \text{ mag}$  brighter luminosities such as to edge any MS+MS star pair in case of unresolved binary systems. See the text for details.

(A color version of this figure is available in the online journal.)

the overall CMD morphology, a spectral synthesis of the cluster stellar population led Buzzoni et al. (2012) to emphasize the *unique role* of this NGC 6791 as a “morceau” of the metal-rich, evolved stellar populations characterizing the upturn-strong giant ellipticals. This conclusion finds further support from the direct experiments of Dorman et al. (1995) and Buzzoni & González-Lópezzira (2008), where the ultraviolet spectra of the strongest UV-upturn galaxies, together with other integrated spectral features, like the  $H\beta$  strength, were actually reproduced in old metal-rich stellar environments with a relative fraction of 20%–25% of BHB stars superposed on a canonical red HB evolution. As a further piece of evidence, stemming from the analysis of the NGC 6791 CMD, one may also recall the recent works of Bedin et al. (2008) and Twarog et al. (2011), where a similar figure (namely  $\sim 30\% \pm 10\%$ ) is independently found for the fraction of binary stars in this cluster. After matching the membership probability, according to Cudworth proper-motion selection (as cited by Twarog et al. 2011) we also confirm this special feature of the NGC 6791 stellar population, as shown in Figure 15. In order to minimize the field-star contamination, we restricted the stellar sample in the figure to only those stars in our catalog within a  $2.5$  radius from the cluster center. A “redward-blurred” distribution is clearly evident for the MS, with brighter and redder outliers nicely comprised within an upper envelope  $0.75 \text{ mag}$  brighter than the fiducial MS locus, as expected for these stars to be MS+MS star pairs. Such a sizeable presence of binary systems has actually been thought, by Bedin et al. (2008), to have begun the WD peculiar distribution as observed for this cluster. If this is the case, then the apparent “excess” of EHB stars may actually be regarded as the key connection between MS and WD evolution.

Although clearly lacking any relevant hot stellar component, clusters NGC 6819 and 7142 might add further arguments on the same line. For both systems, a vanishing and less concentrated low-MS stellar distribution (see Figures 10 and 13) could be one possible consequence of an extended presence of binary

<sup>10</sup> Note, however, that we are somewhat biased against the selection of very bright stars in our photometric catalogs.

(multiple?) stellar systems (the lack of the faintest stars being due, in this case, to their “merging” into the brightest integrated objects). Alternatively, one may call for a disruptive role of Galaxy tides on the dynamical evolution of these open clusters, with the low-mass stars being the most easily stripped objects as a result of Galaxy interaction.

The observation of the surrounding regions along the line of sight of each cluster allows us to usefully probe the Milky Way stellar field at low Galactic latitudes. Our data have been tackled by the theoretical Galaxy model of Girardi et al. (2005), which includes, in some detail, the photometric contribution of all the relevant stellar sub-structures, namely, the spheroid system and the two thin- and thick-disk components. A match of the observed CMDs and *B* luminosity functions across our fields with the theoretical predictions of the model led us to conclude that a more centrally concentrated thick disk (with a scale length shorter than 2.8 kpc, as assumed by Girardi et al. 2005) might better reconcile the lower observed fraction of bright field stars and their WD progeny.

We would like to thank the anonymous referee for a careful reading of the draft and for a number of timely suggestions and recommendations, that greatly helped us in refining our results. A.B. acknowledges the INAOE of Puebla for its warm hospitality, and the European Southern Observatory for awarding a visitorship to ESO premises in Santiago de Chile, where part of this work has been done. This project received partial financial support from the Italian Space Agency ASI, under grant ASI-INAF I/009/10/0 and from the Mexican SEP-CONACyT, under grant CB-2011-01-169554.

*Facility:* TNG

## REFERENCES

- Anthony-Twarog, B. J., Twarog, B. A., & Mayer, L. 2007, *AJ*, 133, 1585  
 Auner, G. 1974, *A&AS*, 13, 143  
 Bedin, L. R., Salaris, M., Piotto, G., et al. 2008, *ApJL*, 679, L29  
 Bertelli, G., Girardi, L., Marigo, P., & Nasi, E. 2008, *A&A*, 484, 815  
 Bragaglia, A., Carretta, E., Gratton, R., et al. 2001, *AJ*, 121, 327  
 Bragaglia, A., & Tosi, M. 2006, *AJ*, 131, 1544  
 Brown, D., Yi, S., Han, Z., & Yoon, S.-J. 2006, *BaltA*, 15, 13  
 Buson, L. M., Bertone, E., Buzzoni, A., & Carraro, G. 2006, *BaltA*, 15, 49  
 Buzzoni, A., Bertone, E., Carraro, G., & Buson, L. M. 2012, *ApJ*, 749, 35  
 Buzzoni, A., & González-Lópezlira, R. A. 2008, *ApJ*, 686, 1007  
 Carney, B. W., Lee, J.-W., & Dodson, B. 2005, *AJ*, 129, 656  
 Carraro, G., & Chiosi, C. 1994, *A&A*, 287, 761  
 Carraro, G., Geisler, D., Villanova, S., Frinchaboy, P. M., & Majewski, S. R. 2007, *A&A*, 476, 217  
 Carraro, G., Girardi, L., & Chiosi, C. 1999, *MNRAS*, 309, 430  
 Carraro, G., Villanova, S., Demarque, P., et al. 2006, *ApJ*, 643, 1151  
 Crinklaw, G., & Talbert, F. D. 1991, *PASP*, 103, 536  
 Dorman, B., O’Connell, R. W., & Rood, R. T. 1995, *ApJ*, 442, 105  
 Girardi, L., Groenewegen, M. A. T., Hatziminaoglou, E., & da Costa, L. 2005, *A&A*, 436, 895  
 Gratton, R., Bragaglia, A., Carretta, E., & Tosi, M. 2006, *ApJ*, 642, 462  
 Jacobson, H. R., Friel, E. D., & Pilachowski, C. A. 2007, *AJ*, 134, 1216  
 Jacobson, H. R., Friel, E. D., & Pilachowski, C. A. 2008, *AJ*, 135, 2341  
 Janes, K. A., & Hoq, S. 2011, *AJ*, 141, 92  
 Kalirai, J. S., Richer, H. B., Fahlman, G. G., et al. 2001, *AJ*, 122, 266  
 Kaluzny, J., & Rucinski, S. M. 1995, *A&AS*, 114, 1  
 Kaluzny, J., & Udalski, A. 1992, *AcA*, 42, 29  
 Kinman, T. D. 1965, *ApJ*, 142, 655  
 Landolt, A. U. 1992, *AJ*, 104, 340  
 Landsman, W., Bohlin, R. C., Neff, S. G., et al. 1998, *AJ*, 116, 789  
 Liebert, J., Saffer, R. A., & Green, E. M. 1994, *AJ*, 107, 1408  
 Lindoff, U. 1972, *A&AS*, 7, 497  
 McLaughlin, D. E., & Fall, S. M. 2008, *ApJ*, 679, 1272  
 Mighell, K. J., Sarajedini, A., & French, R. S. 1998, *AJ*, 116, 2395  
 Montgomery, K. A., Janes, K. A., & Phelps, R. L. 1994, *AJ*, 108, 585  
 Origlia, L., Rood, R. T., Fabbri, S., et al. 2007, *ApJL*, 667, L85  
 Origlia, L., Valenti, E., Rich, R. M., & Ferraro, F. R. 2006, *ApJ*, 646, 499  
 Platais, I., Cudworth, K. M., Kozhurina-Platais, V., et al. 2011, *ApJL*, 733, L1  
 Rosvick, J. M., & Vandenberg, D. A. 1998, *AJ*, 115, 1516  
 Schlegel, D. J., Finkbeiner, D. P., & Davis, M. 1998, *ApJ*, 500, 525  
 Stetson, P. B. 1987, *PASP*, 99, 191  
 Twarog, B. A., Ashman, K. M., & Anthony-Twarog, B. J. 1997, *AJ*, 114, 2556  
 Twarog, B. A., Carraro, G., & Anthony-Twarog, B. J. 2011, *ApJL*, 727, L7  
 van den Bergh, S. 1962, *JRASC*, 56, 41  
 van den Bergh, S., & Heeringa, R. 1970, *A&A*, 9, 209  
 van Loon, J. T. 2006, in ASP Conf. Ser. 353, *Stellar Evolution at Low Metallicity: Mass Loss, Explosions, Cosmology*, ed. H. J. G. L. M. Lamers, N. Langer, T. Nugis, & K. Annuk (San Francisco, CA: ASP), 211  
 von Braun, K., & Mateo, M. 2001, *AJ*, 121, 1522  
 Warren, S. R., & Cole, A. A. 2009, *MNRAS*, 393, 272  
 Yong, H., Demarque, P., & Yi, S. 2000, *ApJ*, 539, 928